Front. Optoelectron. 2021, 14(4): 450–458
https://doi.org/10.1007/s12200-020-1024-0

REVIEW ARTICLE

Recent progress in the research on using $CuSbS_2$ and its derivative $CuPbSbS_3$ as absorbers in case of photovoltaic devices

Muyi ZHANG[1,2], Chong WANG[1], Chao CHEN (✉)[1], Jiang TANG[1,2,3]

1 Sargent Joint Research Center, Wuhan National Laboratory for Optoelectronics, Huazhong University of Science and Technology, Wuhan 430074, China
2 China-EU Institute for Clean and Renewable Energy, Huazhong University of Science and Technology, Wuhan 430074, China
3 School of Optical and Electronic Information, Huazhong University of Science and Technology, Wuhan 430074, China

Abstract Thin-film solar cells show considerable application potential as alternative photovoltaic technologies. Cuprous antimony chalcogen materials and their derivatives, represented as $CuSbS_2$ and $CuPbSbS_3$, respectively, exhibit the advantages of low cost, massive elemental abundance, stability, and good photoelectric properties, including a suitable bandgap and large optical absorption coefficient. These advantages demonstrate that they can be used as light absorbers in photovoltaic applications. In this study, we review the major properties, fabrication methods, and recent progress of the performance of the devices containing $CuSbS_2$ and $CuPbSbS_3$. Furthermore, the limitations and future development prospects with respect to the $CuSbS_2$ and $CuPbSbS_3$ solar cells are discussed.

Keywords $CuSbS_2$, $CuPbSbS_3$, properties, fabrication, performance

1 Introduction

Recently, photovoltaic technology utilizing solar energy has been lauded as a clean and renewable energy provider. In particular, crystalline Si (c-Si) and other semiconductors based on thin-film solar cells have been widely explored in photovoltaic technology. Since the single-crystal $CuInSe_2$-based solar cell was first reported in 1975 with a power conversion efficiency (PCE) of 12% [1], Cu-based solar cells have rapidly developed. The series of breakthrough technologies, such as alloying with gallium (Ga), has also improved the device performance. Thus, the new semiconductor $Cu(In,Ga)(S,Se)_2$ (CIGS) has become one of the most promising light-absorber material for photovoltaic application. To date, the CIGS thin-film solar cell has achieved a PCE of more than 23.35% (area of 1 cm^2) [2], which denotes that the thin-film photovoltaic technologies have an impressive future. However, the prices of the raw materials required to develop CIGS, such as indium (In) and gallium (Ga), are increasing because of elemental scarcity. This is hindering the further development of such solar cells. Meanwhile, as a quinary compound, CIGS has low thermodynamic stability, which increases the difficulty of accurately controlling the composition and defects in a CIGS-based system. Therefore, alternative cheap, stable, and Earth-abundant absorber materials with good photoelectric properties are needed for obtaining efficient thin-film solar cells.

The chalcostibite ($CuSbS_2$) semiconductor has attracted attention as a light absorber in solar cells owing to the obvious advantages of being cheap and abundant. As a naturally stable mineral with massive reserves, $CuSbS_2$ is abundant and cheap. The elemental abundances of Cu, Sb, and S are 60, 0.2, and 350 ppm, respectively (1 ppm = 1.0 mg/kg) [3], and can be purchased at 5624, 5456, and 102 US dollar/ton, respectively (data from London Metal Exchange (LME)). In terms of cost and reserve, $CuSbS_2$ is clearly superior to In, Ga, Se, Cd, and Te in the conventional photovoltaic absorbers, i.e., CIGS and CdTe (Fig. 1**)**. The nontoxicity of $CuSbS_2$ is a further advantage in commercial applications. As a ternary compound, $CuSbS_2$ is similar to $CuInSe_2$ but exhibits better properties in case of photovoltaic applications. Theoretical simulations and experimental results have confirmed a suitable direct bandgap in $CuSbS_2$ (1.38–1.5 eV), indicating the high efficiency limit of single-junction solar cells [4–7]. Further, the spectroscopic limited maximum efficiency (SLME) was calculated; thus, the

Received March 22, 2020; accepted March 31, 2020

E-mail: cchen@mail.hust.edu.cn

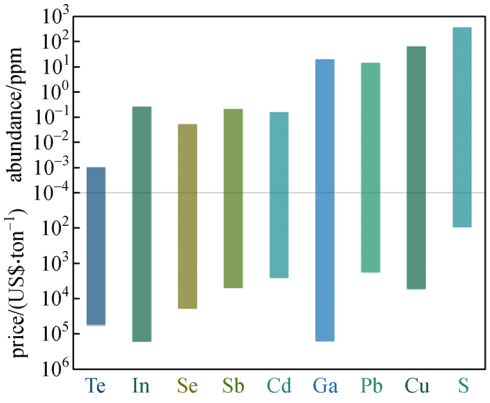

Fig. 1 Comparison of the elemental abundance versus price

theoretical efficiency limit of $CuSbS_2$ was observed to be greater than that of $CuInSe_2$ by 23% when the absorber thickness was 0–500 nm [8]. In addition, due to the $5s^2$ lone pair electron effect on Sb^{3+}, the electronic transition probability from orbits d to p and s to p effectively increased, leading to a higher optical absorption coefficient when compared with that of $CuInSe_2$. Accordingly, the $CuSbS_2$ semiconductor material has received much focus as the light absorber.

With the increasing exploration of the $CuSbS_2$ absorber, its derivative, bournonite ($CuPbSbS_3$), has also drawn considerable attention. $CuPbSbS_3$ is derived from a $CuSbS_2$ system in which a PbS structure is incorporated, resulting in the three-dimensional (3D) crystal structure of $CuPbSbS_3$. This new semiconductor is abundantly available and stable. Pb has a natural abundance of 14 ppm and costs 1878 US dollar/ton in the market, achieving lower-cost photovoltaics than CIGS and CdTe (Fig. 1). $CuPbSbS_3$ possesses a suitable direct bandgap, a larger optical absorption coefficient than that of $CuSbS_2$, and other good photoelectric properties [9]. In addition, the melting points of $CuPbSbS_3$ and $CuSbS_2$ are 522°C and 551°C, respectively [10,11], considerably lower than that of CIGS (1070°C) [12]. Therefore, micron-sized grains of $CuPbSbS_3$ and $CuSbS_2$ are easily obtained at sintering temperatures of 300°C–400°C [13–15], indicating the possibility of low-temperature and large-scale manufacturing that would reduce the cost of photovoltaic applications.

Herein, we will review the major factors associated with $CuSbS_2$ and $CuPbSbS_3$, including their photoelectric properties and stabilities, and the recent progress with respect to photovoltaic devices. The future developmental potential and limitations of photovoltaic technologies are also discussed.

2 Material properties

2.1 Crystal structure and electronic dimensionality

$CuSbS_2$ is an orthorhombic system having a two-dimensional (2D) layered structure comprising twisted Cu–S pentahedra and Sb–S tetrahedra. Each unit cell contains four Cu atoms, four Sb atoms, and eight S atoms, where the Sb atom is three-coordinated with the surrounding S atoms and the Cu atom is four-coordinated with the S atoms (Fig. 2). The lattice parameters are a = 6.018 Å, b = 3.796 Å, c = 14.495 Å, and $\alpha = \beta = \gamma = 90°$. The 2D monolayered crystal structure prevents the overlap of the electron clouds between the layers, allowing efficient transportation of the carriers in an intra-layer manner but blocking their transportation along the out-of-plane direction. Consequently, the transportation of carriers is limited within $CuSbS_2$.

To construct a 3D crystal structure and achieve better transportation of the carriers, the strategy of incorporating PbS into $CuSbS_2$ is proposed [13]. After the incorporation of PbS, $CuSbS_2$ transforms to the new phase of $CuPbSbS_3$, where an orthorhombic system is maintained but the dimensionality of the crystal structure is altered from 2D to 3D (bulk; Fig. 2). The $CuPbSbS_3$ structure comprises twisted Cu–S pentahedra, Pb–S octahedra, and Sb–S tetrahedra. Each unit cell contains four Cu atoms, four Pb atoms, four Sb atoms, and twelve S atoms. The lattice parameters are a = 8.153 Å, b = 8.692 Å, c = 7.793 Å, and $\alpha = \beta = \gamma = 90°$ [10,16]. Within such a 3D structure, the carriers can move in all the directions, improving the transportation properties of $CuPbSbS_3$.

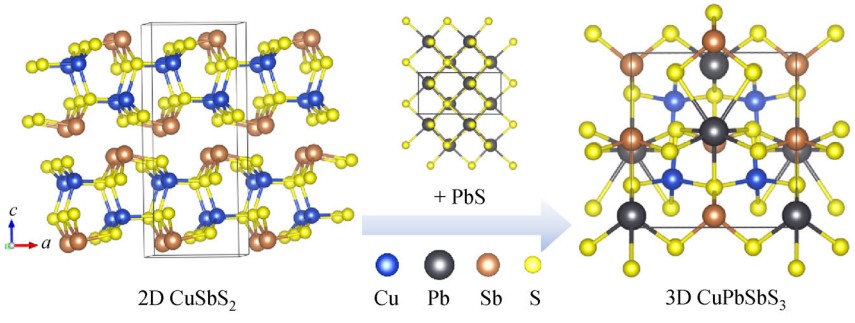

Fig. 2 Crystal structures of $CuSbS_2$ and $CuPbSbS_3$

It is better to account for the photovoltaic properties, such as bandgap, via electronic dimensionality than via structural dimensionality [17]. A high electronic dimensionality is preferred in case of high-performance photovoltaic absorber materials, whereas a 3D crystal structure is a requirement for ensuring high electronic dimensionality. As a 2D structural material, the electronic dimensionality of $CuSbS_2$ is restricted. However, the 3D $CuPbSbS_3$ is expected to demonstrate advanced electronic dimensionality.

The band structure obtained via density functional theory (DFT) **(**Fig. 3**)** was demonstrated to explain the electronic dimensionality of $CuPbSbS_3$. The conduction band minimum (CBM) and valence band maximum (VBM) connect three-dimensionally and disperse along all the directions, confirming 3D electronic dimensionality and leading to the transportation of mobile charge carriers along all the directions. The high electronic dimensionality of $CuPbSbS_3$ enables an isotropic current flow and improved performance. Therefore, $CuPbSbS_3$ is a promising semiconductor absorber in high-efficiency solar cells.

2.2 Optical absorption and band energy

Previous theoretical studies have predicted that $CuSbS_2$ and $CuPbSbS_3$ have good optical absorption. Meanwhile, their absorption coefficients were obtained by fitting to the experimental transmission spectra. The absorption coefficient α is related to the transmission T as

$$\alpha = \frac{\ln(1/T)}{d}, \tag{1}$$

where d is the thickness of the material. Figures 4(a) and 4(b) show the fitting results over the range of visible wavelengths, where the absorption coefficients of $CuSbS_2$ and $CuPbSbS_3$ exceed 7×10^4 and 4×10^5 cm^{-1}, respectively. These absorption coefficients are higher than those of most photovoltaic absorbers, demonstrating that the $CuSbS_2$- and $CuPbSbS_3$-based devices achieve high photoelectric conversion with nanometer-scale thickness.

The experimental bandgaps of $CuSbS_2$ and $CuPbSbS_3$ have been fitted using the absorption coefficient α. The fitting curves (Figs. 4(a) and 4(b) inset) demonstrate bandgap values of 1.4 and 1.31 eV, respectively, which are in agreement with the previous theorical values [11,13,18]. Hoang and Mahanti comprehensively considered multiple factors, including the bandgap, material absorption spectrum, and non-radiative transition, and reported that the maximum theoretical efficiency of $CuSbS_2$ solar cells can exceed 23% [8]. Meanwhile, the bandgap of $CuPbSbS_3$ (1.31 eV) is suitable with respect to solar cell absorbers. According to the relation between the bandgap and maximum efficiency of solar cells, this value could possibly foreshadow the optimal efficiency limit of 33% [19].

$CuSbS_2$ and $CuPbSbS_3$ were subjected to ultraviolet photoelectron spectroscopy (UPS) for determining the band energy (Figs. 4(c) and 4(d)). The Fermi energies E_F of $CuSbS_2$ and $CuPbSbS_3$ are 4.86 eV (ultraviolet photon energy: 21.2 eV, He–I excitation). The linear fittings of the UPS spectra of $CuSbS_2$ and $CuPbSbS_3$ in the long tails generate extrapolations of 0.39 and 0.38 eV, respectively, which correspond to the distance between E_F and VBM. The band energy could be calculated according to bandgaps of 1.4 and 1.31 eV. $CuSbS_2$ has the VBM at -5.25 eV and CBM at -3.85 eV, whereas $CuPbSbS_3$ has the VBM at -5.24 eV and CBM at -3.93 eV. In addition, $CuSbS_2$ and $CuPbSbS_3$ have been confirmed as p-type semiconductors. Owing to their band energy structures, $CuSbS_2$ and $CuPbSbS_3$ easily match with the major buffer layers such as CdS. Table 1 summarizes the common material parameters and properties of $CuSbS_2$ and $CuPbSbS_3$.

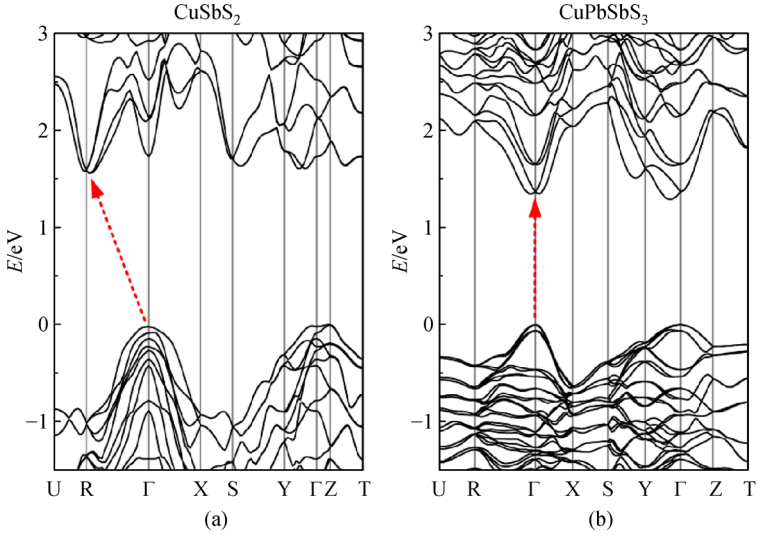

Fig. 3 Band structures of (a) $CuSbS_2$ and (b) $CuPbSbS_3$ obtained via DFT [13]. Copyright 2020. Reproduced with permission from Elsevier

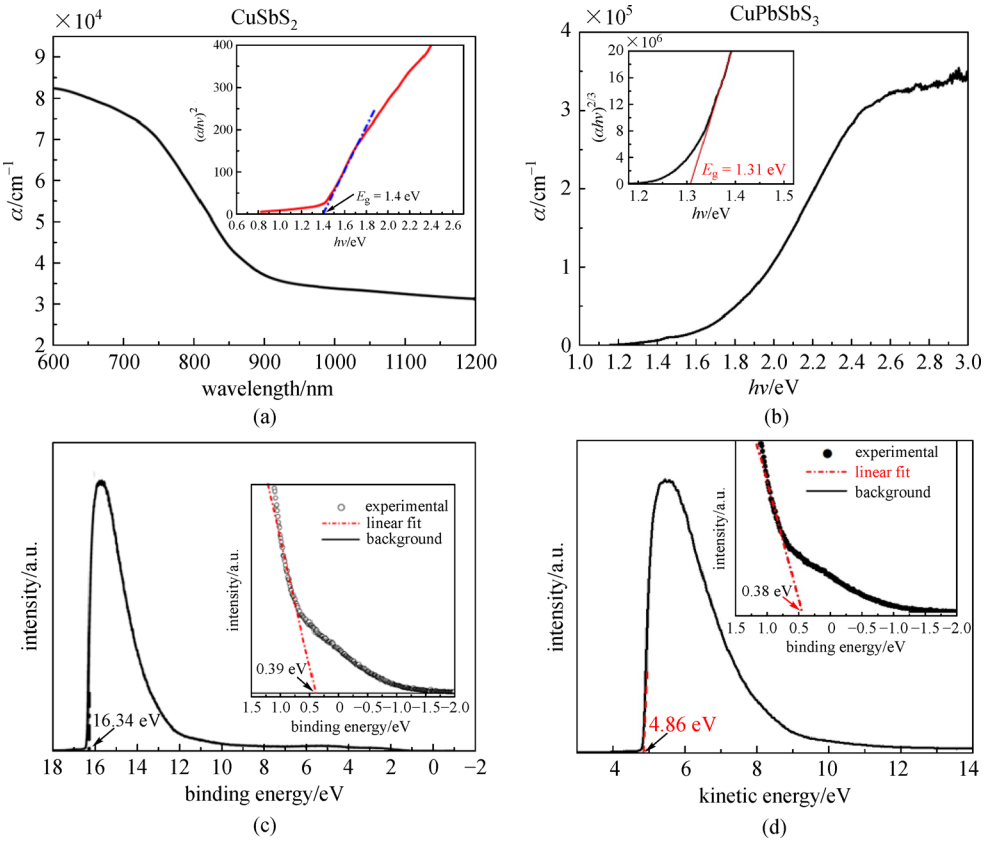

Fig. 4 (a) and (b) Optical absorption coefficients of $CuSbS_2$ and $CuPbSbS_3$, and their linear fittings that are extrapolated to the bandgaps (insets). (c) and (d) UPS spectra of $CuSbS_2$ and $CuPbSbS_3$. Insets show the magnified low-energy spectra and their linear fittings [11,13]. Copyright 2014. Reproduced with permission from ACS Publications; copyright 2020. Reproduced with permission from Elsevier

2.3 Stability

As natural minerals, $CuSbS_2$ and $CuPbSbS_3$ are stable on Earth, indicating their stable physical and chemical properties, including thermal stability, moisture stability, and oxygen stability.

The thermogravimetric analysis (TGA) curves were employed to explain the thermal stability. Figure 5 shows the phase change process with temperature. Below 220°C, the Cu–Sb–S precursor of $CuSbS_2$ was endothermically decomposed via a two-stage process: evaporation of free hydrazine and dissociation of the hydrazinium species at

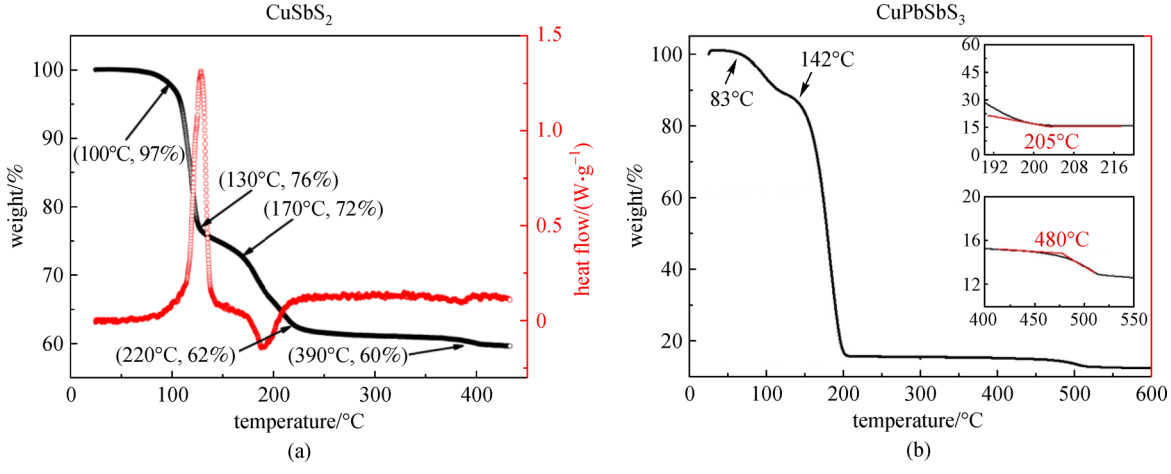

Fig. 5 TGA curves of (a) $CuSbS_2$ powder and (b) $CuPbSbS_3$ solution [11,13]. Copyright 2014. Reproduced with permission from ACS Publications; copyright 2020. Reproduced with permission from Elsevier

100°C–130°C and removal of excess sulfur at 130°C–220°C. This decomposition was followed by stable grain/film formation at 220°C–390°C. Meanwhile, $CuPbSbS_3$ decomposed by the dissociation of the Cu/Pb/Sb complex and volatilization of the organic solvent before 205°C, followed by stable grain/film formation from 205°C to 480°C. These processes demonstrate that $CuSbS_2$ and $CuPbSbS_3$ formed stable grains and steady films at 390°C and 480°C, respectively, indicating their high thermal stability.

In case of photovoltaic absorbers, one major factor is chemical stability, which depends on their reaction with the environment (oxygen, moisture, UV light, etc.). The perovskite solar cells deliver high performance but suffer from severe instability [20], mainly because perovskite is sensitively degraded by moisture and oxygen. Exposure to UV light would promote the decomposition of perovskite. In contrast, $CuSbS_2$ and $CuPbSbS_3$ resist decomposition and environmental reactions under normal conditions because their elements and valences are stable. Although Cu is monovalent in these compounds, the steady Cu–Sb–(Pb)–S bonds resist oxidization. Moreover, all these compositions are barely soluble in water. Therefore, both these materials present high chemical stability.

Furthermore, the device stability has been confirmed based on the aforementioned physically and chemically stable properties. Banu et al. evaluated the stability of the $CuSbS_2$ solar cells [21]. The PCE did not decrease after 3.5 months in an air atmosphere and slightly increased after 7 months of air storage. The stability of the $CuPbSbS_3$ solar cells has also been evaluated [13]. The PCE decreased from 2.23% to 1.80% after one month in air, mainly owing to the poor air stability of the Spiro-OMeTAD hole transport layer.

3 Device fabrication and performance

Until now, the mainstream and effective methods for preparing $CuSbS_2$ films and devices are the vacuum and solution methods. Vacuum methods were employed to produce the $CuSbS_2$ film some time back. In 2008, Rabhi et al. fabricated $CuSbS_2$ film via a single-source vacuum thermal evaporation method [22]. The $CuSbS_2$ powder evaporated and deposited on unheated glass in vacuum, and the film was then annealed at 200°C for 2 h. Without the high-temperature heat treatment, the film exhibited an amorphous structure during characterization analysis. The $CuSbS_2$ film became polycrystalline only after annealing at temperatures of greater than 200°C. Although the fabrication is complex, this vacuum evaporation method achieved large-scale and uniform fabrication. In 2011, Garza et al. proposed a new evaporation method [23], in which the Cu film was deposited onto the Sb_2S_3 film formed by chemical bath deposition (CBD) on glass. After the Cu film was deposited by thermal evaporation, the Sb_2S_3/Cu layer was

Table 1 Material and optoelectronic properties of $CuSbS_2$ and $CuPbSbS_3$

		$CuSbS_2$	$CuPbSbS_3$
mineral species		chalcostibite	bournonite
crystal system		orthorhombic	orthorhombic
space group		*Pnma* (No. 62)	$Pmn2_1$ (No. 31)
lattice parameter/Å	*a*	6.018	7.885
	b	3.796	8.287
	c	14.495	8.816
crystal structure		2D layer	3D network
electronic dimensionality		< 3D	3D
absorption coefficient/cm^{-1} (visible wavelength)		$> 7 \times 10^4$	$> 4 \times 10^5$
bandgap/eV		1.40	1.31
maximum efficiency limit		23%	33%
CBM/eV		−3.85	−3.93
VBM/eV		−5.25	−5.24
Fermi energy/eV		−4.86	−4.86
conduction type		p	p
hole mobility/($cm^2 \cdot v^{-1} \cdot s^{-1}$)		49	7
carrier concentration/cm^{-3}		2.66×10^{18}	6.08×10^{14}
dielectric constant		~13	7.1–7.6
melting point/°C		551	522
density/($g \cdot cm^{-3}$)		5.03	5.63

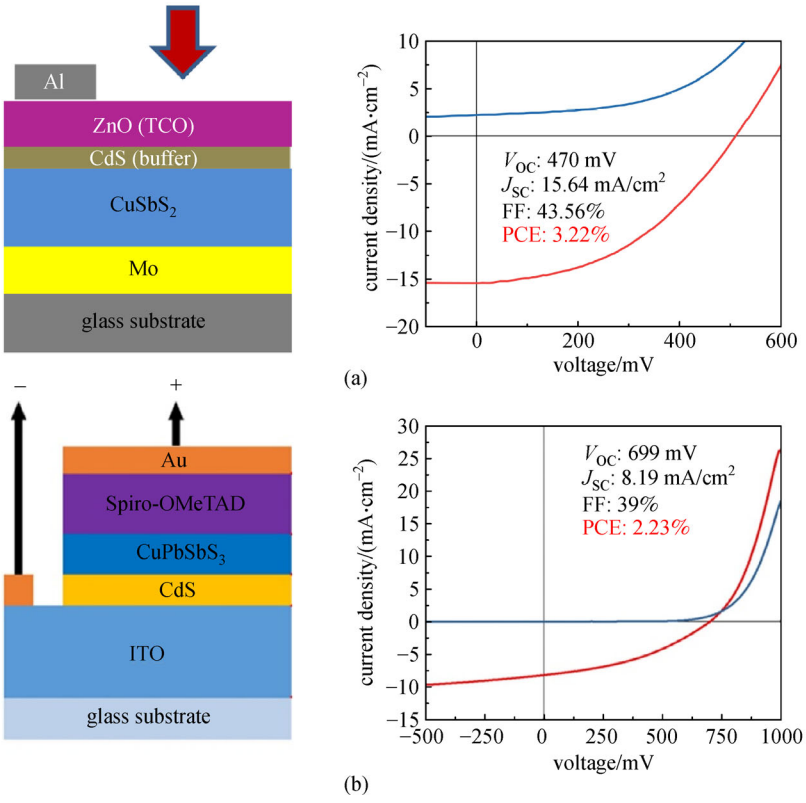

Fig. 6 (a) $CuSbS_2$ device structure exhibiting the best performance until now. (b) $CuPbSbS_3$ device structure exhibiting the best performance until now [13,21]. Copyright 2016 and 2020. Reproduced with permission from Elsevier

annealed at 300°C–380°C. The XRD result showed that the Sb_2S_3/Cu layer would transform to the pure orthorhombic $CuSbS_2$ film during the high-temperature annealing process. Meanwhile, the Hall effect measurements were performed to confirm the p-type conductivity of $CuSbS_2$. Wan et al. subsequently proposed a two-stage co-evaporation process to obtain the film and construct an efficient device [24]. In this process, an Sb-rich precursor was deposited by co-evaporating Cu, Sb, and S at a low substrate temperature (230°C). Sb and S were then co-evaporated at a higher temperature (370°C) to obtain the film. This process improves the crystallinity and phase purity of the $CuSbS_2$ film. When constructed into a solar cell device having a structure of Mo/$CuSbS_2$/CdS/ZnO/ZnO:Al/Ag, the film achieved an encouraging PCE of 1.9% with a high open-circuit voltage (V_{OC}) of 526 mV. The co-sputtering processes for $CuSbS_2$ were recently explored by Saragih et al. [25]. They obtained a $CuSbS_2$ film layer on the TiN-coated Mo/glass substrate by the co-sputtering technique at 300°C, with a Cu and Sb_2S_3 cermet target at 50–60 W and a Cu metal target at 2 W, and annealing was subsequently performed at 350°C–450°C for 1 h. Based on the application of GaN and $In_{0.15}Ga_{0.85}N$ as n-type bilayers, a solar cell device was constructed, achieving a PCE of 2.99%. Welch et al. successfully fabricated a $CuSbS_2$ film after magnetron co-sputtering of the Cu_2S and Sb_2S_3 targets [26].

The solution methods were utilized to produce films and devices. The first complete photovoltaic device based on a $CuSbS_2$ absorber was fabricated via CBD in 2005. This device achieved a V_{OC} of 345 mV and a J_{SC} of 0.2 mA·cm^{-2}, which mean the first observable photovoltaic performance of $CuSbS_2$ solar cell [27]. Since that time, solution preparation methods for $CuSbS_2$ films and devices have proliferated, delivering encouraging performances. Some of the existing solution methods include spray pyrolysis, electrodeposition, and spin coating. Using a precursor of $CuCl_2 \cdot 2H_2O$, $(CH_3COO)_3Sb$, and H_2NCSNH_2 (as the sulfur source) in an aqueous solution, Manolache et al. deposited a $CuSbS_2$ film by the spray pyrolysis process at 240°C [28]. The resulting film was free of pinholes and rich in antimony. In a demonstration of electrochemical deposition, Septina et al. [29] first deposited Cu in an electrolyte containing $CuSO_4$ and citric acid and then deposited an Sb layer in an electrolyte containing $K_2(Sb_2(C_4H_2O_6)_2)$, and tartaric acid. After deposition, the metal precursor was sulfurized under H_2S flow, forming $CuSbS_2$. This approach yielded a solar cell with a glass/Mo/$CuSbS_2$/CdS/ZnO:Al structure, a PCE of 3.13%, and a high V_{OC} (490 mV). Spin coating is the most effective method for fabricating efficient devices. In 2016, Banu et al. constructed a glass/Mo/$CuSbS_2$/CdS/i-ZnO/n-ZnO/Al structure with a PCE of 3.22% [21], which was the highest PCE reported in $CuSbS_2$ solar cells at that time

Table 2 Fabrication methods and performances of the efficient $CuSbS_2$ and $CuPbSbS_3$ devices (PCEs > 1.9%) developed since 2014

absorber	device structure	fabrication	V_{OC}/mV	J_{SC}/(mA·cm^{-2})	FF/%	PCE/%	year	Ref.
$CuSbS_2$	glass/Mo/$CuSbS_2$/CdS/ZnO:Al	electrochemical deposition	490	14.73	44	3.13	2014	[29]
$CuSbS_2$	glass/FTO/TiO_2/mp-TiO_2/$CuSbS_2$/HTM/Au	metal/thiourea + spin coating	304	21.50	46.8	3.10	2015	[31]
$CuSbS_2$	glass/Mo/$CuSbS_2$/CdS/ZnO/ZnO:Al/Ag	two-stage co-evaporation	526	9.57	37.4	1.90	2016	[24]
$CuSbS_2$	glass/Mo/$CuSbS_2$/CdS/i-ZnO/n-ZnO/Al	spin coating	470	15.64	43.56	3.22	2016	[21]
$CuSbS_2$	glass/Mo/TiN/$CuSbS_2$/GaN/$In_{0.15}Ga_{0.85}N$/ITO	co-sputtering	295	33.78	30	2.99	2017	[25]
$CuPbSbS_3$	glass/ITO/CdS/$CuPbSbS_3$/HTM/Au	BDCA solution + spin coating	699	8.19	39	2.23	2020	[13]

(Fig. 6(a)). Further, some treatments, such as post-annealing treatments, have been explored to improve the performance of the $CuSbS_2$-based solar cells [30].

The device applications of the $CuPbSbS_3$ derivative were first proposed several decades ago. In 1973, Frumar et al. synthesized the first single-crystal $CuPbSbS_3$ and studied its physical properties [10]. Recently, Tablero explored the optical properties of $CuPbSbS_3$ and proposed its usage in photovoltaic applications [9]. Also, Liu et al. reported the first $CuPbSbS_3$ solar cell with a glass/ITO/CdS/$CuPbSbS_3$/Spiro-OMeTAD/Au structure. This cell was produced in solution via the spin coating process [13]. The new butyldithiocarbamate (BDCA, $C_5H_{11}NS_2$) solution method prepares a high-quality $CuPbSbS_3$ precursor, yielding a high-performance device after spin coating and annealing. This device achieves a PCE of 2.23% and a V_{OC} of 699 mV (Fig. 6(b)). Table 2 summarizes the developmental progress of efficient devices (with PCEs > 1.9%) based on the $CuSbS_2$ and $CuPbSbS_3$ solar cells since 2014.

4 Future developments and limitations

$CuSbS_2$ and $CuPbSbS_3$ are promising absorber materials in photovoltaic applications. Their main materials and photoelectric properties have been proved previously, but the exploration of devices is in the initial stages.

Owing to their different material properties, $CuSbS_2$ and $CuPbSbS_3$ have unique advantages and disadvantages. The simplicity of components, high hole mobility, and large dielectric constant of $CuSbS_2$ make it a better absorber candidate than $CuPbSbS_3$; as such, the former has attracted more attention. However, the high doping concentration causes excessive conductivity and degenerates the semiconductor behavior; moreover, the low electronic dimensionality of the 2D monolayered crystal structure constrains the transportation of charge carriers. $CuPbSbS_3$ is promising because of its large optical absorption coefficient, optimal bandgap, suitable doping concentration, and other beneficial properties; however, its further development must overcome two major hurdles, i.e., the difficulty of controlling and fabricating complex quaternary components and the toxicity of Pb. These problems may be overcome via the usage of advanced fabrication processes in the future. For example, device encapsulation may be a solution to prevent toxicity. Moreover, the large Pb atoms increase the density of $CuPbSbS_3$ and improve the absorption of high-energy photons. Therefore, this material is expected to be used in future X-ray detection applications.

With regard to device fabrication, $CuSbS_2$ and $CuPbSbS_3$ devices with the highest performances were fabricated via the solution process followed by spin coating. The components of ternary and quaternary compounds are better controlled by the solution methods than by the vacuum methods. However, the solution methods introduce more defects than the vacuum methods and decrease the transportation ability of the formed film. These problems can seriously limit the device performance. Although solution methods can become the future direction of device fabrication, decreasing the defects and improving the transportation of charge carriers within the absorber film are demanded.

5 Conclusions

The cuprous antimony disulfide ($CuSbS_2$) and its derivative, cuprous lead antimony trisulfide ($CuPbSbS_3$), are cheap, abundant, and stable. Furthermore, they exhibit good photoelectric properties, indicating their potential for application as light absorbers in future photovoltaic technologies. Solar cell devices have been developed based on these materials, and excellent performances have been achieved, encouraging further research and applications. We believe that further explorations will lead to new breakthroughs with respect to device performance. The cuprous antimony chalcogen materials and their derivative, represented by $CuSbS_2$ and $CuPbSbS_3$, respectively, are expected to become research hotspots in case of photovoltaic technologies.

Acknowledgements This work was financially supported by the National Natural Science Foundation of China (Grant Nos. 61725401, and 61904058), the National Key R&D Program of China (No. 2016YFA0204000), the China Postdoctoral Science Foundation (Nos. 2018M642825 and 2019M662623), the National Postdoctoral Program for Innovative Talent (No. BX20190127), and the HUST Key Innovation Team for Interdisciplinary Promotion (Nos. 2016JCTD111 and 2017KFXKJC003). The authors would also like to thank the Analytical and Testing Center of HUST and the facility support of the Center for Nanoscale Characterization and Devices (CNCD), WNLO, HUST.

Conflicts of Interest The authors declare no conflict of interest.

References

1. Shay J, Wagner S, Kasper H. Efficient $CuInSe_2$/CdS solar cells. Applied Physics Letters, 1975, 27(2): 89–90
2. Nakamura M, Yamaguchi K, Kimoto Y, Yasaki Y, Kato T, Sugimoto H. Cd-free Cu(In,Ga)$(Se,S)_2$ thin-film solar cell with record efficiency of 23.35%. IEEE Journal of Photovoltaics, 2019, 9(6): 1863–1867
3. Haynes W M, Lide D R. Abundance of Elements in the Earth's Crust and in the Sea. CRC Handbook of Chemistry and Physics. 95th edition, Internet Version. CRC Press, 2014
4. Rodriguez-Lazcano Y, Nair M, Nair P.$Cu_xSb_yS_z$ thin films produced by annealing chemically deposited Sb_2S_3-CuS thin films. Modern Physics Letters B, 2001, 15(17n19): 667–670
5. Rodríguez-Lazcano Y, Nair M, Nair P. $CuSbS_2$ thin film formed through annealing chemically deposited Sb_2S_3–CuS thin films. Journal of Crystal Growth, 2001, 223(3): 399–406
6. Shockley W, Queisser H J. Detailed balance limit of efficiency of p-n junction solar cells. Journal of Applied Physics, 1961, 32(3): 510–519
7. Zhou J, Bian G Q, Zhu Q Y, Zhang Y, Li C Y, Dai J. Solvothermal crystal growth of $CuSbQ_2$ (Q = S, Se) and the correlation between macroscopic morphology and microscopic structure. Journal of Solid State Chemistry, 2009, 182(2): 259–264
8. Hoang K, Mahanti S D. Atomic and electronic structures of IV–VI_2 ternary chalcogenides. Journal of Science: Advanced Materials and Devices, 2016, 1(1): 51–56
9. Tablero C. The optical properties of $CuPbSbS_3$-bournonite with photovoltaic applications. Theoretical Chemistry Accounts, 2016, 135(5): 126
10. Frumar M, Kala T, Horak J. Growth and some physical properties of semiconducting $CuPbSbS_3$ crystals. Journal of Crystal Growth, 1973, 20(3): 239–244
11. Yang B, Wang L, Han J, Zhou Y, Song H, Chen S, Zhong J, Lv L, Niu D, Tang J. $CuSbS_2$ as a promising earth-abundant photovoltaic absorber material: a combined theoretical and experimental study. Chemistry of Materials, 2014, 26(10): 3135–3143
12. Tinoco T, Rincón C, Quintero M, Pérez G S. Phase diagram and optical energy gaps for $CuIn_yGa_{1-y}Se_2$ alloys. Physica Status Solidi (a), 1991, 124(2): 427–434
13. Liu Y, Yang B, Zhang M, Xia B, Chen C, Liu X, Zhong J, Xiao Z, Tang J. Bournonite $CuPbSbS_3$: an electronically-3D, defect-tolerant, and solution-processable semiconductor for efficient solar cells. Nano Energy, 2020, 71: 104574
14. Majsztrik P, Kirkham M, Garcia-Negron V, Lara-Curzio E, Skoug E, Morelli D. Effect of thermal processing on the microstructure and composition of Cu–Sb–Se compounds. Journal of Materials Science, 2013, 48(5): 2188–2198
15. Zhang Y, Ozolins V, Morelli D, Wolverton C. Prediction of new stable compounds and promising thermoelectrics in the Cu–Sb–Se system. Chemistry of Materials, 2014, 26(11): 3427–3435
16. Edenharter A, Nowacki W, Takéuchi Y. Verfeinerung der Kristallstruktur von Bournonit $[(SbS_3)_2|Cu^{IV2}Pb^{VII}Pb^{VIII}]$ und von Seligmannit $[(AsS_3)_2|Cu_2^{IV}Pb^{VII}Pb^{VIII}]$. Zeitschrift für Kristallographie. Crystalline Materials, 1970, 131(1–6): 397–417
17. Xiao Z, Meng W, Wang J, Mitzi D B, Yan Y. Searching for promising new perovskite-based photovoltaic absorbers: the importance of electronic dimensionality. Materials Horizons, 2017, 4(2): 206–216
18. Temple D J, Kehoe A B, Allen J P, Watson G W, Scanlon D O. Geometry, electronic structure, and bonding in $CuMCh_2$ (M = Sb, Bi; Ch = S, Se): alternative solar cell absorber materials? Journal of Physical Chemistry C, 2012, 116(13): 7334–7340
19. Rühle S. Tabulated values of the Shockley–Queisser limit for single junction solar cells. Solar Energy, 2016, 130: 139–147
20. Niu G, Guo X, Wang L. Review of recent progress in chemical stability of perovskite solar cells. Journal of Materials Chemistry A, Materials for Energy and Sustainability, 2015, 3(17): 8970–8980
21. Banu S, Ahn S J, Ahn S K, Yoon K, Cho A. Fabrication and characterization of cost-efficient $CuSbS_2$ thin film solar cells using hybrid inks. Solar Energy Materials and Solar Cells, 2016, 151: 14–23
22. Rabhi A, Kanzari M, Rezig B. Growth and vacuum post-annealing effect on the properties of the new absorber $CuSbS_2$ thin films. Materials Letters, 2008, 62(20): 3576–3578
23. Garza C, Shaji S, Arato A, Tijerina E P, Castillo G A, Roy T D, Krishnan B. p-Type $CuSbS_2$ thin films by thermal diffusion of copper into Sb_2S_3. Solar Energy Materials and Solar Cells, 2011, 95(8): 2001–2005
24. Wan L, Ma C, Hu K, Zhou R, Mao X, Pan S, Wong L H, Xu J. Two-stage co-evaporated $CuSbS_2$ thin films for solar cells. Journal of Alloys and Compounds, 2016, 680: 182–190
25. Saragih A D, Kuo D H, Tuan T T A. Thin film solar cell based on p-$CuSbS_2$ together with Cd-free GaN/InGaN bilayer. Journal of Materials Science Materials in Electronics, 2017, 28(3): 2996–3003
26. Welch A W, Zawadzki P P, Lany S, Wolden C A, Zakutayev A. Self-regulated growth and tunable properties of $CuSbS_2$ solar absorbers. Solar Energy Materials and Solar Cells, 2015, 132: 499–506
27. Rodríguez-Lazcano Y, Nair M, Nair P. Photovoltaic pin structure of Sb_2S_3 and $CuSbS_2$ absorber films obtained via chemical bath deposition. Journal of the Electrochemical Society, 2005, 152(8): G635–G638
28. Manolache S, Duta A, Isac L, Nanu M, Goossens A, Schoonman J. The influence of the precursor concentration on $CuSbS_2$ thin films deposited from aqueous solutions. Thin Solid Films, 2007, 515(15): 5957–5960
29. Septina W, Ikeda S, Iga Y, Harada T, Matsumura M. Thin film solar cell based on $CuSbS_2$ absorber fabricated from an electrochemically deposited metal stack. Thin Solid Films, 2014, 550: 700–704
30. Zhang Y, Huang J, Yan C, Sun K, Cui X, Liu F, Liu Z, Zhang X, Liu

X, Stride J A, Green M A, Hao X. High open-circuit voltage $CuSbS_2$ solar cells achieved through the formation of epitaxial growth of $CdS/CuSbS_2$ hetero-interface by post-annealing treatment. Progress in Photovoltaics: Research and Applications, 2019, 27(1): 37–43

31. Choi Y C, Yeom E J, Ahn T K, Seok S I. $CuSbS_2$ -sensitized inorganic-organic heterojunction solar cells fabricated using a metal-thiourea complex solution. Angewandte Chemie International Edition, 2015, 54(13): 4005–4009

Muyi Zhang received his B.E. degree from the China University of Petroleum in 2017. He is currently pursuing his M.S. degree from both the Huazhong University of Science and Technology (China) and the MINES ParisTech of PSL University (France). He is involved in studying photoelectric materials and devices, including X-ray detectors and thin-film solar cells, at the Wuhan National Laboratory for Optoelectronics.

E-mail: sxyzzhangmuyi@gmail.com

Chong Wang, a Ph.D. candidate at the Wuhan National Laboratory for Optoelectronics (WNLO), Huazhong University of Science and Technology (HUST), majors in Optical Engineering. He received his Bachelor's degree from HUST in 2015. His current research interests include novel semiconductor optoelectronic materials and devices.

E-mail: wangchong2015@hust.edu.cn

Dr. **Chao Chen** received his B.Sc. degree from the School of Physics of the Huazhong University of Science and Technology in June 2014. From September 2014 to February 2019, he studied at the Wuhan National Laboratory for Optoelectronics of the Huazhong University of Science and Technology as a doctoral candidate and received his Ph.D. degree in February 2019. Currently, he is a postdoctoral fellow at the Wuhan National Laboratory for Optoelectronics of the Huazhong University of Science and Technology. His research interests include thin-film solar cells and photodetectors.

E-mail: cchen@mail.hust.edu.cn

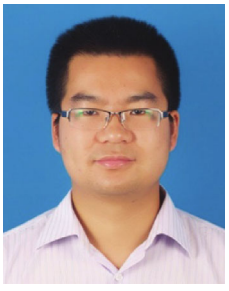

Prof. **Jiang Tang** received his B.Sc. degree (2003) from the University of Science and Technology of China and Ph.D. (2010) from the University of Toronto under the supervision of Prof. Edward Sargent. After one and a half years of postdoctoral research at the IBM T.J. Watson Research Center, he joined the Wuhan National Laboratory for Optoelectronics, Huazhong University of Science and Technology, as a full-time professor. His research interests include exploration of new semiconductors for optoelectronic devices. Specifically, he pioneered antimony selenide (Sb_2Se_3) thin-film solar cells, constructed lead-free halide perovskite X-ray detectors with a low detection limit, and developed stable and efficient white emissive halide perovskites. He has published more than 100 papers in renowned journals, including *Nature*, *Nature Materials*, *Nature Photonics*, *Nature Energy*, and *Nature Communications*, and has accumulated more than 9000 citations. He is one of the Executive Editors-in-Chief of *Frontiers of Optoelectronics* and an Editorial Advisor Board member of *Solar RRL*. Further, he has delivered more than 50 invited or plenary talks at various international conferences and prestigious universities.

E-mail: jtang@hust.edu.cn